Antenna measurements using a hologram CATR

T. Sehm, J. Ala-Laurinaho, T. Hirvonen and A.V. Räisänen

It becomes increasingly difficult to obtain far-field measurements for large millimetre wave antennas at higher frequencies due to the required large distance between the antennas. A hologram compact antenna test range (CATR) is used to determine the radiation characteristics of a 39GHz planar antenna in a small facility. The results are compared with those obtained from planar near-field scanning and conventional far-field measurements.

Introduction: For large millimetre wave antennas, the required far-field distances may be up to tens of kilometres, which makes indoor far-field measurements impossible. Variable weather conditions and interfering signals are disadvantages of outdoor measurement facilities. Compact antenna test ranges (CATRs) and near-field measurements can be used to overcome these problems. In a CATR, a spherical wave is transformed into a plane wave in a small space by using a collimating element, e.g. a reflector, lens, or hologram [1, 2]. The antenna under test (AUT) is illuminated with this plane wave. The radiation characteristics of an antenna can also be derived from the near-field by using a Fourier transform [3]. To determine the near-field of the AUT, samples of the field are taken along a predefined surface using a probe. In this Letter, planar near-field scanning and hologram CATR techniques are studied in a practical measurement situation and the results are compared with those obtained previously from far-field measurements.

The AUT is presented in [4]. The AUT is a linearly polarised antenna array with 256 radiating elements. The AUT aperture in the E-field direction is about 32cm long and in the H-field direction 25cm. A gain of 37dBi and the E- and H-plane radiation patterns have been measured outdoors using gain comparison and far-field measurement techniques at a distance of ~25m at 39.3GHz. Since the far-field requirement for this antenna is 20m, it is not possible to perform the far-field measurements indoors at the Helsinki University of Technology. This is the reason for studying alternatives to the far-field method, even for the measurement of such a small antenna operating at a rather low frequency.

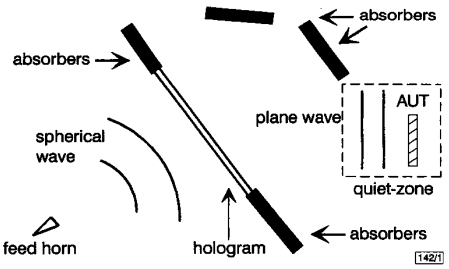

Fig. 1 *Hologram CATR*

Hologram CATR: Fig. 1 illustrates a measurement facility layout employing a hologram CATR. The feed horn transmits a spherical wave onto one side of a computer-generated amplitude hologram structure, which modulates the field such that a planar wave is emanated on the other side of the structure. The planar wave is designed to leave at an angle of 33° to avoid disturbance of the diffraction wavemodes propagating in the direction of the hologram normal. The AUT is illuminated by the plane wave. The extent of the volume enclosing the plane wave is called the quiet-zone. The required field quality of the quiet-zone is driven by the required measurement accuracy of the AUT. Typical requirements are a peak-to-peak amplitude ripple < 1dB and a peak-to-peak phase ripple < 10° in the quiet-zone [2].

Another benefit is the straightforward measurement method, where no post-processing is required. This is not the case for near-field scanning methods, where the measurement and post-processing times may be of the order of hours [3]. A hologram based CATR is intended especially for short millimetre and submillimetre-wave frequencies, where the surface accuracy requirements for reflectors, which are commonly used in CATRs, are becoming very stringent [5]. Furthermore, the manufacturing costs of a hologram are much lower than for a reflector, which creates a similar quiet-zone field.

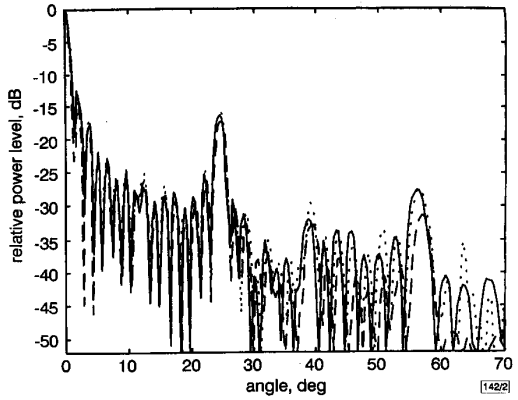

Fig. 2 *Measured E-plane radiation pattern at 39.3GHz*

——— far-field
— — near-field
- - - - hologram

A transmitting amplitude hologram, such as that used here for the compact range, can be realised by an appropriately shaped thin metal pattern etched on a dielectric film. In this application, the size of the hologram is 1.5m × 1.4m ($W \times H$) and it is made on 75μm thick Mylar film with a 17μm copper layer on top. The hologram is made of three pieces joined together, since it could not be manufactured in one piece. The length of the facility is ~6.5m and the width is 3m. A corrugated horn is used as the feed. The hologram design is presented in more detail in [2, 6]. The simulated quiet-zone field has an amplitude ripple of < 0.5dB peak-to-peak and a phase ripple < 5° peak-to-peak. The quality of the quiet-zone was tested by a horn attached to a computer controlled linear scanner. The amplitude of the co- and cross-polar quiet-zone fields were measured in the vertical and horizontal directions at various positions. The width of the quiet-zone is 70cm, the height is 45cm, and the measured peak-to-peak amplitude ripple is ~2.1dB. The main reasons for the increased ripple compared to the simulated result are the manufacturing errors of the hologram: etching errors of the slots and misalignment of the three pieces of the hologram, also reported in [5]. The room used for the hologram measurement is an ordinary laboratory facility with concrete walls. To reduce reflections from the walls and to prevent the feed radiating directly to the quiet-zone, a large amount of absorbers were used. Critical spots are the structure supporting the hologram, the direction of the hologram normal and the direction 33° from the normal opposite the quiet-zone, and the direct radiation path, as indicated in Fig. 1. However, reflections could not be completely prevented, which together with the manufacturing errors, increased the quiet-zone ripple.

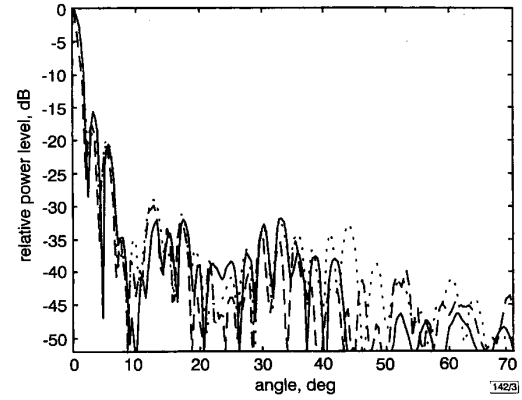

Fig. 3 *Measured H-plane radiation pattern at 39.3 GHz*

——— far-field
— — near-field
- - - - hologram

Since the aperture of the AUT is smaller than the quiet-zone, the position of the AUT within the quiet-zone can be varied. The AUT positions in the quiet-zone were chosen so that the ripple was < 1.3dB. The measured radiation patterns are presented in Figs. 2 and 3. The results are in good agreement with those obtained in the far-field down to sidelobes ~30dB below peak. At lower levels, the ripple in the quiet-zone, and the reflections from the surroundings and the structure supporting the hologram, affect the measured power level. The quality of the quiet-zone can be improved by using an anechoic chamber and by separating the left side (see Fig. 1) from the right side with a wall. The gain comparison technique with a 20dBi standard gain horn was used to determine the AUT gain. The AUT gain measured with the hologram CATR at 39.3GHz is ~35dBi, which is 2dB lower than the gain measured in the far-field.

Planar near-field scanning: The planar near-field scanning facility used consists of inverted H-type translation gear, a HP8510 vector network analyser, and a personal computer. The computer controls the network analyser and the movements of the translation gear. An open-ended WR-28 waveguide probe is attached to the translation gear, forming the transmitting section of the setup. At each sampling point, the copolar amplitude and phase are measured. Absorbing material is placed around the probe and the AUT as well as in the surroundings of the facility to eliminate reflections. With a 23dB amplifier in the transmitting port of the vector network analyser, the output power was ~6dBm at 39.3GHz. However, due to the attenuation of the flexing cables and the insertion loss between the probe and the AUT, the dynamic range is only ~30dB.

The post-processing consisting of the near-field to far-field transformation was carried out using software from Orbit Advanced Technology. The software contains a mathematical model for open-ended waveguides, which was used in the probe correction calculations. At a distance of 3.8cm 211 × 219 samples were taken with a spacing of 3.3mm ($\simeq 0.43\lambda$) in both planes. The number of samples corresponds to an angular region of validity of -80° .... 80° in both principal planes [7]. The number of samples determines the processing gain resulting from the near-field to far-field conversion. The amount of processing gain is equal to the square root of the number of samples, which in this case gives ~47dB [3]. The results of the near-field measurements are compared to the results obtained from far-field and hologram CATR measurements in Figs. 2 and 3. The radiation patterns agree with the results obtained with the other methods. The dynamic range and the phase variations in the flexing cables limit the measurement accuracy of sidelobe levels to < -30dB. The gain measurement is carried out by comparing the gain of the AUT with the gain of a standard gain horn [7]. The measured gain for the AUT is 37.1dBi. The uncertainty of the gain measurement is of the order of a few tenths of a dB [7], thus it is in good agreement with the gain of 37dBi measured in the far-field.

Conclusion: The radiation characteristics of a 39GHz planar array have been measured using a hologram based CATR, planar near-field scanning, and conventional far-field techniques. The results agree well down to sidelobe levels 30–35dB below peak. The measured gain in the far-field and planar near-field scanning agree. The measured gain in the hologram CATR is affected by an overly quiet-zone ripple and reflections from the surroundings. The hologram CATR has been tested and its suitability for antenna measurements also at long millimetre wavelengths has been demonstrated. The dimensions of a hologram CATR are significantly smaller than for a far-field range, thus enabling indoor measurements to be carried out.

22 March 1999
Electronics Letters Online No: 19990557
DOI: 10.1049/el:19990557

T. Sehm, J. Ala-Laurinaho, T. Hirvonen and A.V. Räisänen (*Radio Laboratory/Institute of Radio Communications, Helsinki University of Technology, PO Box 3000, FIN-02015 HUT, Finland*)

References

1 OLVER, A.D.: 'Compact antenna test ranges'. Proc. Seventh Int. Conf. Antennas and Propagation (ICAP), York, UK, 1991, pp. 99–108

2 HIRVONEN, T., ALA-LAURINAHO, J., TUOVINEN, J., and RÄISÄNEN, A.V.: 'A compact antenna test range based on a hologram', *IEEE Trans.*, 1997, **AP-45**, (8), pp. 1270–1276

3 SLATER, D.: 'Near-field measurements' (Artech House, Boston, 1991), p. 310

4 SEHM, T., LEHTO, A., and RÄISÄNEN, A.V.: 'A large planar antenna consisting of an array of waveguide fed horns', *IEEE Trans.*, 1998, **AP-46**, (8), pp. 1189–1193

5 HIRVONEN, T., ALA-LAURINAHO, J., LEHTO, A., TUOVINEN, J., and RÄISÄNEN, A.V.: 'Feasibility of a hologram CATR for measuring large mm- and submm-wave antennas'. Proc. 20th ESTEC Antenna Workshop on Millimetre Wave Antenna Technology and Antenna Measurement, Noordwijk, 1997, pp. 355–362

6 ALA-LAURINAHO, J., HIRVONEN, T., TUOVINEN, J., and RÄISÄNEN, A.V.: 'Numerical modeling of a non-uniform grating with the FDTD', *Microw. Opt. Technol. Lett.*, 1997, **15**, (3), pp. 134–139

7 NEWELL, A.C.: 'Error analysis techniques for planar near-field measurements', *IEEE Trans.*, 1988, **AP-36**, (6), pp. 754–768

Broadband FDTD analysis of infinite phased arrays using periodic boundary conditions

H. Holter and H. Steyskal

A new technique for the FDTD analysis of periodic infinite phased arrays is presented. Periodic boundary conditions are implemented which reduce the computational volume to that of a single unit cell. The technique applies to pulse scanning in oblique directions and is performed by continuously moving the unit cell in the scan plane.

Introduction: In the frequency domain, the mathematical treatment of infinite arrays is greatly simplified by Floquet's theorem, which reduces the analysis to that of a single unit cell in the array. However, unit cell analysis in the time domain is complicated for the following reason. Consider a unit cell ABCD with dimension $D_x \times D_y$ in an infinite periodic array, as shown in Fig. 1, and assume that the array is scanned in the $y = 0$ plane to an angle θ in the positive x-direction. The fields at boundaries C and D are then identical at every point of time. Therefore, simple time independent boundary conditions can be applied. However, at boundaries A and B the tangential fields are related according to

$$f(x_B, y, z, t) = f(x_A, y, z, t - \tau_x) \quad (1)$$

$$f(x_A, y, z, t) = f(x_B, y, z, t + \tau_x) \quad (2)$$

where $\tau_x = D_x \sin\theta / c$ is the time delay between adjacent unit cells and c is the speed of light. Eqn. 1 implies that tangential field values at boundary B are obtained from time delayed values at boundary A, which are simply saved in a buffer for later use. On the other hand, eqn. 2, implies that time advanced field values from boundary B are used at boundary A. This poses a major problem, since the time advanced values at time $\tau + \tau_x$ are not known at time t.

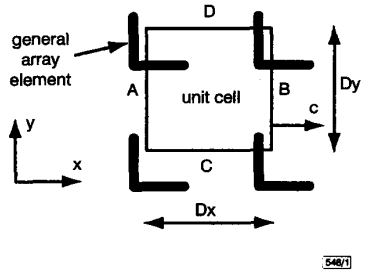

Fig. 1 *Section of infinite array aperture*